International Journal of Recent Technology and Engineering (IJRTE)
ISSN: 2277-3878 (Online), Volume-10 Issue-6, March 2022

A Contact Type Three-Dimensional Position Measuring Instrument for Verification of a Piping Inspection Robot

Hirofumi Maeda

Abstract*: Since 1965, the sewerage system development have been promoted in Japan, but as the number of management facilities has increased, the number of facilities that have been used for a long time has also increased, and nowadays, they are too old for daily operation. Because of this problem, the maintenance of drainage and sewer pipes have been carried out continuously. However, in-pipe inspection has a wide inspection range and is a harsh task for operating personnel, which leads to actively-performed inspections using robots in recent years. Under the circumstances mentioned above, the stand-alone type of robot, which can inspect piping by itself, is becoming the mainstream at present. We have focused on the capability of embedding downsized yet high performance PCs and sensors. In recent years, we have been studying and developing robots with those capabilities on board for piping inspection. However, for the inspection using the robot, there is always the risk that the robot itself tips over due to the undulation of the pipe joint and the slip caused by sludge. Therefore, we devised a self-position estimation in absolute coordinates using only an accelerometer in order to achieve highly accurate straight-ahead control for preventing tip over as a software approach without relying on hardware approach such as tire replacement or similar methods. Currently, we are in the stage of verifying this self-position estimation, and for that purpose, we need an instrument for measuring the position of the robot. Therefore, in this paper, we propose the structure of the measuring instrument that does not significantly disturb the driving of the robot due to the disturbance caused via the connection part of the piping inspection robot and the measuring instrument. In addition, as a result of experiments, even in the initial state where the accuracy of the measuring instrument is not calibrated, the average translation error is within 0.58 mm, the average angle error is within 0.12 degree, the standard deviation of the translation error is within 0.86 mm, and the standard deviation of the angle error is within 2.67 degree. It is shown that it can be used for verification of the robot.

***Keywords*: Measuring Instrument, Contact Type, Exploration Robot, Localization, Water Pipe**

I. INTRODUCTION

Since 1965, sewerage systems development has been promoted in Japan, but as the number of management facilities has increased, the number of facilities that have been used for a long time has also increased, and nowadays they are too old for daily operation. The standard service life of a sewer pipe is 50 years, and the risk of the road collapse increases 30 years after the pipe is laid. Therefore, the maintenance of drainage is a harsh task for operating personnel, which leads to actively-performed inspections using robots [1].

In a typical piping inspection robot, a carrier for operation is installed near the manhole, and only the self-propelled vehicle, which is the main body of the robot and tethered to the carrier, is put into the piping, and operated remotely. With this method, not only can the weight of the robot body be reduced by mounting only the minimum functions required for driving, excluding the control unit and power supply unit, on the self-propelled vehicle, but also can be controlled and monitored by the operator on the ground, which enables the operator to react to the unforeseen circumstances immediately. On the other hand, it requires a lot of labor and cost, such as securing a place to install a carrier and securing personnel for wide-area intrusion regulation at the time of inspection. Furthermore, since the entire system is large-scale, it is necessary to secure enough funding for running costs and personnel for maintenance.

Therefore, the stand-alone type, which can inspect piping by itself, is becoming the mainstream at present. Its type is inexpensive and is easy to carry, so it has the great feature of being able to inspect multiple pipes at the same time. This type of robots has been developed all over the world, but since the standard pipe diameter outside Japan is 200 mm or more, it cannot be used for pipes with a diameter of 150 mm, which are required to be inspected in Japan. In Japan, although many studies and development of this type of robot have been widely carried out, there are still few of them that can be used for Japanese standard diameter regardless of where they are made [2]-[5]. Under these circumstances, we have focused on the capability of embedding downsized yet high performance PCs and sensors. In recent years, we have been studying and developing robots with those capabilities on board for piping inspection. With particular emphasis on reducing the burden on inspectors, we have aimed to put into practical use a compact and easy-to-carry autonomous piping inspection robot that utilizes the know-how of rescue robots that we have developed so far [6]-[13]. In the process of studies, we devised the idea to develop a modular-type robot that can be assembled without screws for the purpose of improving maintainability, which was inspired by the “secret box,” which is one of the traditional Japanese crafts “Hakone wooden mosaic work.” [14] Apart from this, for the inspection using the robot, there is always the risk that the robot itself tips over due to the undulation of the pipe joint and the slips caused by sludge.

Manuscript received on February 16, 2022.
Revised Manuscript received on February 21, 2022.
Manuscript published on March 30, 2022.
* Correspondence Author
Hirofumi Maeda*, Information Science and Technology Department, National Institute of Technology (KOSEN), Yuge College, Ehime Prefecture, Japan. Email: maeda@info.yuge.ac.jp

With the remote-control method via a cable, as mentioned above, the state of the robot is constantly controlled and monitored through the monitor, enabling the operator to immediately respond to unexpected situations including falls. On the other hand, in the stand-alone type, it is necessary to equip the robot body with all the functions, and not only the inspection process but also the preventive system for avoiding the tip over must be incorporated into it. As a way to prevent this tip over, conventional pipe inspection robots have adopted a tire replacement or similar hardware approach as a method of matching the size of the robot body to the diameter of inspected pipes. However, this approach not only requires time for replacing tires before and after inspection due to hardware changes, but also has many problems such as damage or loss when changing parts, transportation of tools used for necessary changes, and cost of the changed parts themselves. Therefore, we decided to aim for highly accurate straight-ahead control for preventing tip over as software approach without relying on tire replacement or similar hardware-based methods. In order to realize this control, highly accurate self-position estimation is critical. Under normal circumstances, the estimation is possible using accelerometers, gyro sensors, and geomagnetic sensors. However, in the underground piping like this time, the robot body is easy to slip and the magnetic field is strong, so there are many situations where the gyro sensor and geomagnetic sensor are unreliable. Therefore, in order to avoid unexpected slips or tip-over, or to perform zero position correction by resetting the robot, we devised a self-position estimation in absolute coordinates using only an accelerometer [15].

Currently, we are in the stage of verifying this estimation, and equipment for measuring the position of the robot is needed for that purpose. However, in order to measure the position and posture in a pipe, a three-dimensional position measuring instrument, which is expensive and large-scale, is required. Therefore, we decided to develop an inexpensive and highly accurate three-dimensional position measuring instrument for piping inspection robots. Three-dimensional position measuring instruments are roughly divided into non-contact type and contact type. The non-contact type has a wide measurement range and does not cause disturbance to target objects, but the accuracy is lower than that of the contact type. In addition, since it does not physically touch the target object, it is not damaged easily and can be used for any target regardless of its materials. On the other hand, since the contact type directly touches the target object, the measurement result is accurate and reliable. However, in addition to the disadvantages mentioned above compared to the non-contact type, the contact type can be more complex in terms of the structure, and physically less durable with many comparative parts, making the system itself more complex. For this reason, we have developed a non-contact three-dimensional position measuring instrument using ARToolKit [16]. This measuring instrument was three-dimensionally calibrated by a virtual 9-axis manipulator considering the tilt errors caused by hardware installation and machining. As a result, we succeeded in greatly improving the measurement accuracy, but due to problems such as camera resolution, we could not achieve the accuracy in the depth direction, which is the z-axis [17]-[18].

Therefore, in this paper, we propose the structure of the measuring instrument that does not significantly disturb the driving of the robot due to the disturbance caused via the connection part of the piping inspection robot and the measuring instrument. In addition, the details of the measuring instrument for verifying the robot are described, focusing on its structure. Finally, the accuracy verification results of the measuring instrument obtained by the experiment are also described.

II. THE CONTACT-TYPE THREE-DIMENSIONAL POSITION MEASURING INSTRUMENT

To verify a pipe inspection robot, the test field using a pipe cut in half as shown in Figure 1 is used. The contact type three-dimensional position measuring instrument is hung directly above the piping, which is the test field. The specific structure and system configuration of the measuring instrument are shown below.

Fig. 1 The Test Field for Verification of a Piping Inspection Robot

A. Structure of the Measuring Instrument

Figure 2 shows the appearance of the measuring instrument. The measuring instrument is hung from the upper part of the carrier by a frame, and as shown in Figure 3, a 6-axis stage for verifying the accuracy of the measuring instrument is attached to the lower part. The measuring instrument has six encoders attached to each joint. As shown in the link structure in Figure 4, each joint is designated as J_1 to J_6 in order from the mounting frame. J_1, J_2 and J_4 to J_6 are rotary joints, while J_3 is a translational joint. The reason why J_3 is a translational joint is not only to have sufficient displacement of the measuring instrument in the height direction, but also to realize a special structure that eliminates the disturbance described later.

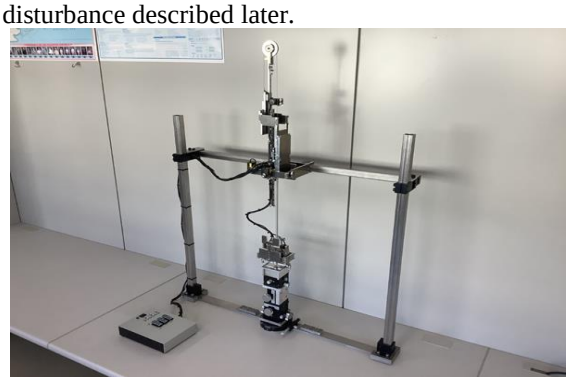

Fig. 2 Exterior of the Contact Type Three-dimensional Position Measuring Instrument

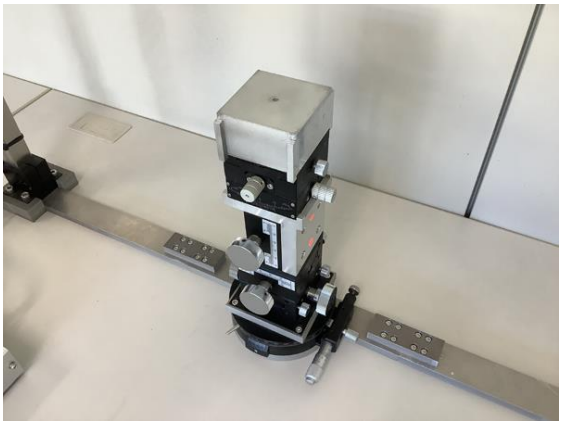

Fig. 3 The 6-axis Stage for Accuracy Verification

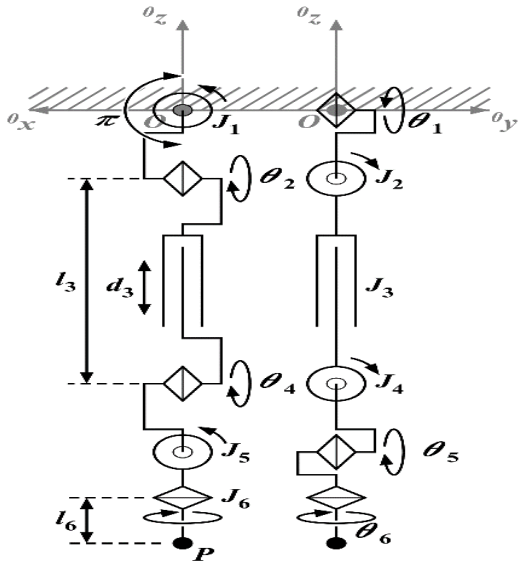

J_1-J_6 : the position of each joint
P : the position of the end effector
$\theta_1, \theta_2, \theta_4$-$\theta_6$: θ_1 to θ_6 excluding θ_3 each indicates the rotation angles for J_1 to J_6 excluding J_3 [rad]
d_3 : d_3 indicates the displacement for J_3 [m]
l_3 : l_3 indicates the initial link length for J_3 [m]
l_6 : link length of the end effector [m]
※ The joint pair of J_1 and J_2 shares the same axis, so do the another joint pair of J_4, J_5 and J_6, which leads to there is no link length between each joint pair.

Fig. 4 Link Structure of the Measuring Instrument

There are two types of disturbance that the measuring instrument gives through the connection part of the robot: "the weight of the measuring instrument on the robot" and "the moment of inertia around the tip of the measuring instrument that is the connection part between the measuring instrument and the robot." As a matter of fact, as long as the measuring instrument touches the robot, the disturbance on the robot cannot be set to zero. However, in the verification of the robot, the disturbance can be ignored if it is reduced to the extent that it does not affect the driving of the robot, making the disturbance sufficiently small with respect to the torque generated by the robot. The structure that reduces the disturbance in terms of hardware is described below.

1. The Weight of the Measuring Instrument on the Robot

There is a constraint that the measuring instrument must be hung from directly above the test field in order to verify the robot. By the method of turning this constraint into the advantage, the weight of the measuring instrument on the robot can be set as much closer as possible to zero.

As shown in Figure 5, a mounting frame is installed to hang the measuring instrument. If the measuring instrument is floating in the air not connected to the robot, the mounting frame takes the weight of the measuring instrument. However, the measuring instrument is put on the robot on the ground, and the weight of the measuring instrument is all taken on the robot.

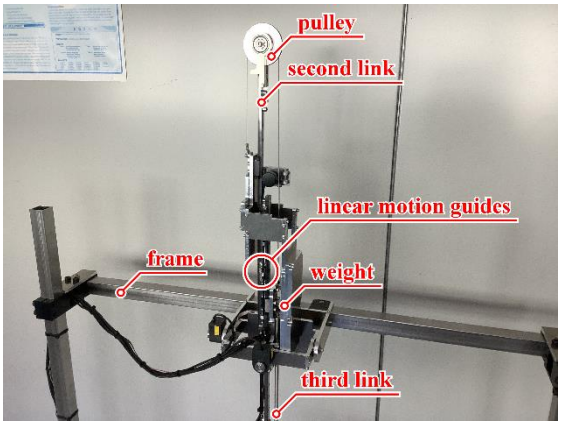

Fig. 5 The Mounting Part of the Measuring Instrument

Therefore, even when the measuring instrument and the robot are connected, this problem can be solved if the structure is such that the weight of the measuring instrument is always taken to the mounting frame. The second link attached to the second joint is mostly composed of linear guides, and a pulley is attached to the upper part (Fig. 5). The third link and a weight are hung from this pulley with a wire. The third link is connected to the tip of the measuring instrument, and the weight is adjusted and attached so that it has the same mass, enabling the third link to be stopped at any place without being affected by gravity. In other words, since twice the mass from the third link to the tip of the measuring instrument is taken to the mounting frame via the second joint, the robot itself does not theoretically take the weight of the measuring instrument itself. However, in reality, the measuring instrument has a hardware error, creating some weight applied to the robot. However, as mentioned above, the disturbance is sufficiently small with respect to the torque generated by the robot, creating no significant effect on running.

2. The Moment of Inertia around the Connection Part between the Measuring Instrument and the Robot

The moment of inertia around the connection between the measuring instrument and the robot is greatly affected by the moment of inertia around each joint.

Here, if the moment of inertia when rotating around the axis passing through the center of gravity of the object is defined as I_c, the distance between the axis of rotation and the axis of the center of gravity of the object is defined as h, and the mass of the object is defined as M, From the parallel axis theorem, the moment of inertia I around the axis of rotation is given by Eq. (1).

$$I = I_c + Mh^2 \quad (1)$$

Therefore, in order to minimize the moment of inertia around the connection between the measuring instrument and the robot, the distance between the rotation axis of each joint and the center of gravity axis of each object should be set to zero. In other words, the axis of rotation of each joint and the axis of the center of gravity of the object are aligned. For that purpose, it is advisable to design while adjusting the balance up to the second joint while providing the weight balances (the counter balances) so that the rotation axes and the center of gravity of the links match in order from the sixth joint. When doing this, after roughly adjusting the mass on the 3D CAD software, the parts are manufactured in order from the sixth joint. Furthermore, efficient processing can be performed by actually weighing and then scraping the parts to adjust the mass.

B. System Configuration

Figure 6 shows the entire system, and Figure 7 shows the control circuit. STK-7125 manufactured by Alpha Project Co., Ltd. is used to acquire the encoder. In addition, the company's STK-7125EVB, which is the debug evaluation board for STK-7125, is used to assist in writing programs to STK-7125. UN-2000 and DX-025 from Mutoh Industries, Ltd. are used as encoders, and the rotation angles are measured from the difference between A phase and B phase in the phase counting mode after connecting to STK-7125 by open collectors. After that, the encoder values obtained by STK-7125 are transferred to the iPad via BLE. Finally, each joint angle is derived and accumulated from the encoder values on the iPad, and the position and posture of the robot are calculated based on the data (Figure 8). The calculation of the robot's position and posture is described in detail in the next chapter.

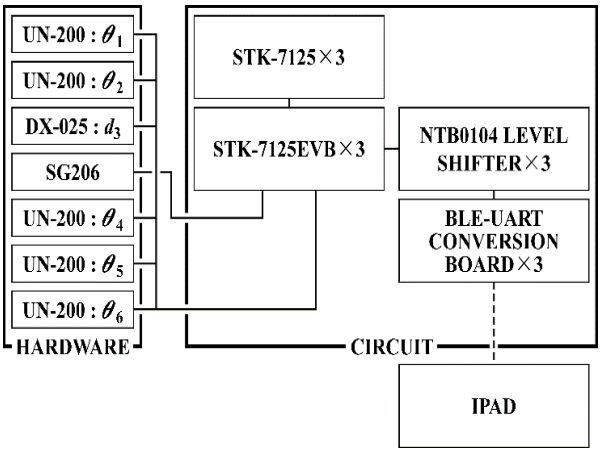

Fig. 6 Schematic Diagram of the System

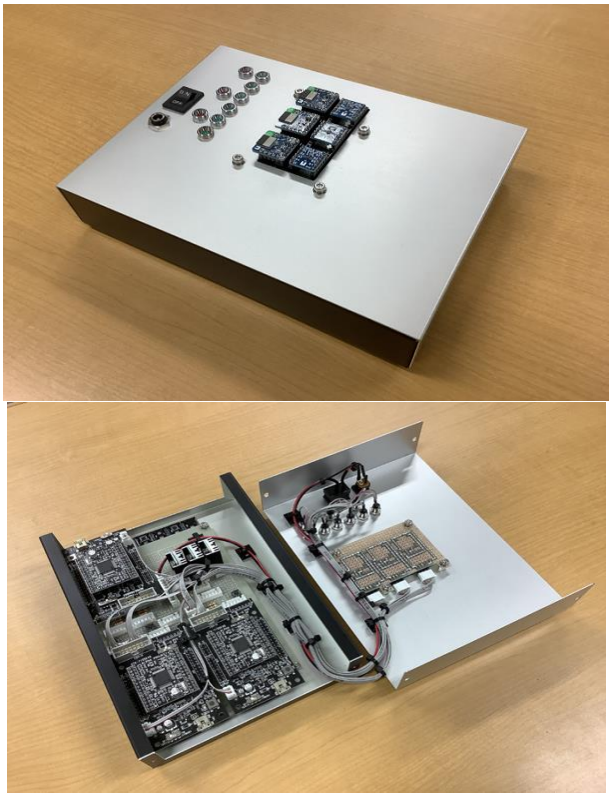

Fig. 7 The Control Circuit of the Measuring Instrument

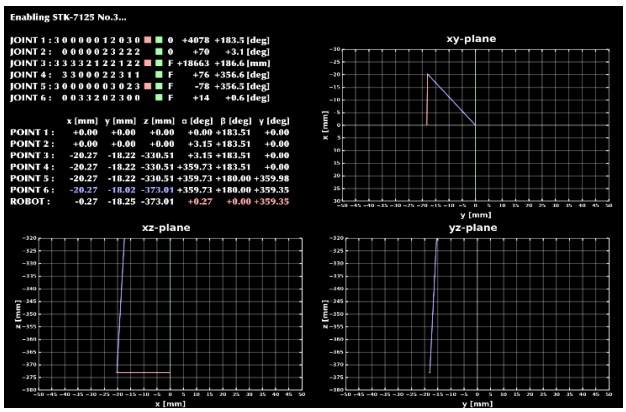

Fig. 8 An Example of the Position and Posture Display Screen

III. MEASUREMENT THEORY

From Fig. 4, translational and rotational movements are performed around the y-axis, around the x-axis, the z-axis direction, around the x-axis, around the y-axis, and around the z-axis from the first joint to the sixth joint, respectively. Therefore, the position and posture of the tip of the measuring instrument can be expressed by Eq. (2) using the homogeneous transformation matrix of forward kinematics. Here, since the measuring instrument is hung from the frame, the initial value is the state of π rad rotation around the y-axis at the origin. Therefore, the first joint angle is $\theta_1+\pi$ [rad].

Next, we consider how to attach the robot to be measured. The robot is mounted with the tip of the measuring instrument rotated by $-\pi/2$ rad around the y-axis. Therefore, the position and posture of the robot is expressed by Eq. (3).

$$\begin{bmatrix} \cos(\theta_1+\pi) & 0 & \sin(\theta_1+\pi) & 0 \\ 0 & 1 & 0 & 0 \\ -\sin(\theta_1+\pi) & 0 & \cos(\theta_1+\pi) & 0 \\ 0 & 0 & 0 & 1 \end{bmatrix} \begin{bmatrix} 1 & 0 & 0 & 0 \\ 0 & \cos\theta_2 & -\sin\theta_2 & 0 \\ 0 & \sin\theta_2 & \cos\theta_2 & 0 \\ 0 & 0 & 0 & 1 \end{bmatrix} \begin{bmatrix} 1 & 0 & 0 & 0 \\ 0 & 1 & 0 & 0 \\ 0 & 0 & 1 & d_3+l_3 \\ 0 & 0 & 0 & 1 \end{bmatrix}$$

$$\begin{bmatrix} 1 & 0 & 0 & 0 \\ 0 & \cos\theta_4 & -\sin\theta_4 & 0 \\ 0 & \sin\theta_4 & \cos\theta_4 & 0 \\ 0 & 0 & 0 & 1 \end{bmatrix} \begin{bmatrix} \cos\theta_5 & 0 & \sin\theta_5 & 0 \\ 0 & 1 & 0 & 0 \\ -\sin\theta_5 & 0 & \cos\theta_5 & 0 \\ 0 & 0 & 0 & 1 \end{bmatrix} \begin{bmatrix} \cos\theta_6 & -\sin\theta_6 & 0 & 0 \\ \sin\theta_6 & \cos\theta_6 & 0 & 0 \\ 0 & 0 & 1 & l_6 \\ 0 & 0 & 0 & 1 \end{bmatrix}$$

$$= \begin{bmatrix} -\cos\theta_1\cos\theta_5\cos\theta_6 \\ -\sin\theta_1\sin(\theta_2+\theta_4)\sin\theta_6 \\ +\sin\theta_1\cos(\theta_2+\theta_4)\sin\theta_5\cos\theta_6 \end{bmatrix} \begin{bmatrix} \cos\theta_1\cos\theta_5\sin\theta_6 \\ -\sin\theta_1\sin(\theta_2+\theta_4)\cos\theta_6 \\ -\sin\theta_1\cos(\theta_2+\theta_4)\sin\theta_5\sin\theta_6 \end{bmatrix} \begin{bmatrix} -\cos\theta_1\sin\theta_5 \\ -\sin\theta_1\cos(\theta_2+\theta_4)\cos\theta_5 \end{bmatrix} \begin{bmatrix} -l_6\cos\theta_1\sin\theta_5 \\ -l_6\sin\theta_1\cos(\theta_2+\theta_4)\cos\theta_5 \\ -(d_3+l_3)\sin\theta_1\cos\theta_2 \end{bmatrix}$$

$$\begin{bmatrix} \cos(\theta_2+\theta_4)\sin\theta_6 \\ +\sin(\theta_2+\theta_4)\sin\theta_5\cos\theta_6 \end{bmatrix} \begin{bmatrix} \cos(\theta_2+\theta_4)\cos\theta_6 \\ -\sin(\theta_2+\theta_4)\sin\theta_5\sin\theta_6 \end{bmatrix} \begin{bmatrix} -\sin(\theta_2+\theta_4)\cos\theta_5 \end{bmatrix} \begin{bmatrix} -l_6\sin(\theta_2+\theta_4)\cos\theta_5 \\ -(d_3+l_3)\sin\theta_2 \end{bmatrix}$$

$$\begin{bmatrix} \sin\theta_1\cos\theta_5\cos\theta_6 \\ -\cos\theta_1\sin(\theta_2+\theta_4)\sin\theta_6 \\ +\cos\theta_1\cos(\theta_2+\theta_4)\sin\theta_5\cos\theta_6 \end{bmatrix} \begin{bmatrix} -\sin\theta_1\cos\theta_5\sin\theta_6 \\ -\cos\theta_1\sin(\theta_2+\theta_4)\cos\theta_6 \\ -\cos\theta_1\cos(\theta_2+\theta_4)\sin\theta_5\sin\theta_6 \end{bmatrix} \begin{bmatrix} \sin\theta_1\sin\theta_5 \\ -\cos\theta_1\cos(\theta_2+\theta_4)\cos\theta_5 \end{bmatrix} \begin{bmatrix} l_6\sin\theta_1\sin\theta_5 \\ -l_6\cos\theta_1\cos(\theta_2+\theta_4)\cos\theta_5 \\ -(d_3+l_3)\cos\theta_1\cos\theta_2 \end{bmatrix}$$

$$\begin{bmatrix} 0 \end{bmatrix} \begin{bmatrix} 0 \end{bmatrix} \begin{bmatrix} 0 \end{bmatrix} \begin{bmatrix} 1 \end{bmatrix} \quad (2)$$

$$\begin{bmatrix} \cos(\theta_1+\pi) & 0 & \sin(\theta_1+\pi) & 0 \\ 0 & 1 & 0 & 0 \\ -\sin(\theta_1+\pi) & 0 & \cos(\theta_1+\pi) & 0 \\ 0 & 0 & 0 & 1 \end{bmatrix} \begin{bmatrix} 1 & 0 & 0 & 0 \\ 0 & \cos\theta_2 & -\sin\theta_2 & 0 \\ 0 & \sin\theta_2 & \cos\theta_2 & 0 \\ 0 & 0 & 0 & 1 \end{bmatrix} \begin{bmatrix} 1 & 0 & 0 & 0 \\ 0 & 1 & 0 & 0 \\ 0 & 0 & 1 & d_3+l_3 \\ 0 & 0 & 0 & 1 \end{bmatrix}$$

$$\begin{bmatrix} 1 & 0 & 0 & 0 \\ 0 & \cos\theta_4 & -\sin\theta_4 & 0 \\ 0 & \sin\theta_4 & \cos\theta_4 & 0 \\ 0 & 0 & 0 & 1 \end{bmatrix} \begin{bmatrix} \cos\theta_5 & 0 & \sin\theta_5 & 0 \\ 0 & 1 & 0 & 0 \\ -\sin\theta_5 & 0 & \cos\theta_5 & 0 \\ 0 & 0 & 0 & 1 \end{bmatrix} \begin{bmatrix} \cos\theta_6 & -\sin\theta_6 & 0 & 0 \\ \sin\theta_6 & \cos\theta_6 & 0 & 0 \\ 0 & 0 & 1 & l_6 \\ 0 & 0 & 0 & 1 \end{bmatrix} \begin{bmatrix} \cos\left(-\frac{\pi}{2}\right) & 0 & \sin\left(-\frac{\pi}{2}\right) & 0 \\ 0 & 1 & 0 & 0 \\ -\sin\left(-\frac{\pi}{2}\right) & 0 & \cos\left(-\frac{\pi}{2}\right) & 0 \\ 0 & 0 & 0 & 1 \end{bmatrix}$$

$$= \begin{bmatrix} -\cos\theta_1\sin\theta_5 \\ -\sin\theta_1\cos(\theta_2+\theta_4)\cos\theta_5 \end{bmatrix} \begin{bmatrix} \cos\theta_1\cos\theta_5\sin\theta_6 \\ -\sin\theta_1\sin(\theta_2+\theta_4)\cos\theta_6 \\ -\sin\theta_1\cos(\theta_2+\theta_4)\sin\theta_5\sin\theta_6 \end{bmatrix} \begin{bmatrix} \cos\theta_1\cos\theta_5\cos\theta_6 \\ +\sin\theta_1\sin(\theta_2+\theta_4)\sin\theta_6 \\ -\sin\theta_1\cos(\theta_2+\theta_4)\sin\theta_5\cos\theta_6 \end{bmatrix} \begin{bmatrix} -l_6\cos\theta_1\sin\theta_5 \\ -l_6\sin\theta_1\cos(\theta_2+\theta_4)\cos\theta_5 \\ -(d_3+l_3)\sin\theta_1\cos\theta_2 \end{bmatrix}$$

$$\begin{bmatrix} -\sin(\theta_2+\theta_4)\cos\theta_5 \end{bmatrix} \begin{bmatrix} \cos(\theta_2+\theta_4)\cos\theta_6 \\ -\sin(\theta_2+\theta_4)\sin\theta_5\sin\theta_6 \end{bmatrix} \begin{bmatrix} -\cos(\theta_2+\theta_4)\sin\theta_6 \\ -\sin(\theta_2+\theta_4)\sin\theta_5\cos\theta_6 \end{bmatrix} \begin{bmatrix} -l_6\sin(\theta_2+\theta_4)\cos\theta_5 \\ -(d_3+l_3)\sin\theta_2 \end{bmatrix}$$

$$\begin{bmatrix} \sin\theta_1\sin\theta_5 \\ -\cos\theta_1\cos(\theta_2+\theta_4)\cos\theta_5 \end{bmatrix} \begin{bmatrix} -\sin\theta_1\cos\theta_5\sin\theta_6 \\ -\cos\theta_1\sin(\theta_2+\theta_4)\cos\theta_6 \\ -\cos\theta_1\cos(\theta_2+\theta_4)\sin\theta_5\sin\theta_6 \end{bmatrix} \begin{bmatrix} -\sin\theta_1\cos\theta_5\cos\theta_6 \\ +\cos\theta_1\sin(\theta_2+\theta_4)\sin\theta_6 \\ -\cos\theta_1\cos(\theta_2+\theta_4)\sin\theta_5\cos\theta_6 \end{bmatrix} \begin{bmatrix} l_6\sin\theta_1\sin\theta_5 \\ -l_6\cos\theta_1\cos(\theta_2+\theta_4)\cos\theta_5 \\ -(d_3+l_3)\cos\theta_1\cos\theta_2 \end{bmatrix}$$

$$\begin{bmatrix} 0 \end{bmatrix} \begin{bmatrix} 0 \end{bmatrix} \begin{bmatrix} 0 \end{bmatrix} \begin{bmatrix} 1 \end{bmatrix} \quad (3)$$

IV. ACCURACY VERIFICATION

The accuracy of the measuring instrument was verified using the 6-axis stage shown in Fig. 3. In the link structure shown in Fig. 4, the parameters of the manufactured measuring instrument are l_3 = 145.0 mm and l_6 = 42.5 mm, and the link structure of the 6-axis stage is shown in Figure 9.

Published By:
Blue Eyes Intelligence Engineering
and Sciences Publication (BEIESP)

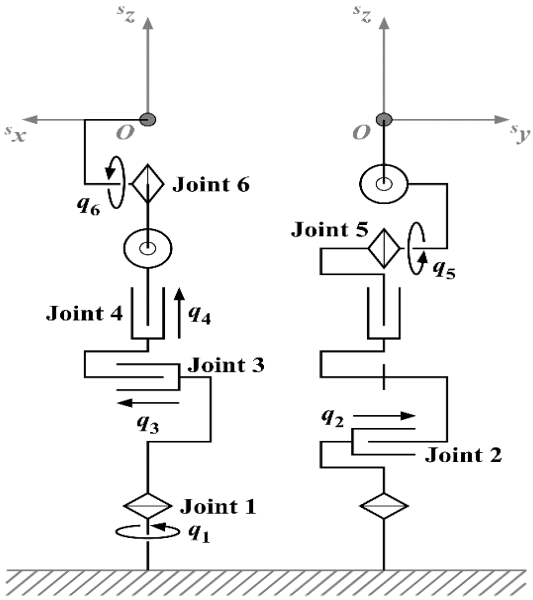

Fig. 9 Link Structure of the 6-axis Stage

Accuracy verification was performed for translation and rotation, respectively. In the verification in translation, 27 patterns of combinations of x = -20.0, 0.0, 20.0 mm, y = -20.0, 0.0, 20.0 mm, z = -373.0, -363.0, -353.0 mm, and $\alpha = \beta = \gamma = 0.0$ degree were performed for the point $\boldsymbol{P}$ (x, y, z, α, β, γ). The rotation was verified using 27 combinations of $x = y = z = 0.0$ mm, α = -15.0, 0.0, 15.0 degree, β = -15.0, 0.0, 15.0 degree, and γ = -15.0, 0.0, 15.0 deg. The results of each experiment are shown in Table 1 and Table 2.

Table 1 Results of Accuracy Verification in Translation

ideal value						measured value						error					
x [mm]	y [mm]	z [mm]	α [deg]	β [deg]	γ [deg]	x [mm]	y [mm]	z [mm]	α [deg]	β [deg]	γ [deg]	x [mm]	y [mm]	z [mm]	α [deg]	β [deg]	γ [deg]
-20.00	-20.00	-373.00	0.00	0.00	0.00	-20.10	-18.87	-373.04	0.18	0.00	-0.10	-0.10	1.13	-0.04	0.18	0.00	-0.10
-20.00	-20.00	-363.00	0.00	0.00	0.00	-20.17	-18.74	-363.07	0.27	0.00	-0.11	-0.17	1.26	-0.07	0.27	0.00	-0.11
-20.00	-20.00	-353.00	0.00	0.00	0.00	-20.28	-18.89	-353.14	0.27	0.00	-0.06	-0.28	1.11	-0.14	0.27	0.00	-0.06
0.00	-20.00	-373.00	0.00	0.00	0.00	-0.33	-19.49	-372.99	0.00	0.09	-0.05	-0.33	0.51	0.01	0.00	0.09	-0.05
0.00	-20.00	-363.00	0.00	0.00	0.00	-0.57	-19.37	-363.00	0.04	0.09	-0.05	-0.57	0.63	0.00	0.04	0.09	-0.05
0.00	-20.00	-353.00	0.00	0.00	0.00	-0.59	-19.23	-353.10	0.09	0.13	0.00	-0.59	0.77	-0.10	0.09	0.13	0.00
20.00	-20.00	-373.00	0.00	0.00	0.00	19.36	-19.92	-373.00	-0.18	0.18	-0.06	-0.64	0.08	0.00	-0.18	0.18	-0.06
20.00	-20.00	-363.00	0.00	0.00	0.00	19.25	-19.77	-363.14	-0.09	0.22	-0.05	-0.75	0.23	-0.14	-0.09	0.22	-0.05
20.00	-20.00	-353.00	0.00	0.00	0.00	19.37	-19.61	-353.06	-0.05	0.22	-0.05	-0.63	0.39	-0.06	-0.05	0.22	-0.05
-20.00	0.00	-373.00	0.00	0.00	0.00	-20.53	0.33	-373.02	0.09	0.00	-0.01	-0.53	0.33	-0.02	0.09	0.00	-0.01
-20.00	0.00	-363.00	0.00	0.00	0.00	-20.42	0.35	-363.09	0.13	0.00	-0.01	-0.42	0.35	-0.09	0.13	0.00	-0.01
-20.00	0.00	-353.00	0.00	0.00	0.00	-20.27	0.07	-353.02	0.09	0.00	-0.01	-0.27	0.07	-0.02	0.09	0.00	-0.01
0.00	0.00	-373.00	0.00	0.00	0.00	-0.29	-0.29	-372.99	-0.05	0.04	-0.04	-0.29	-0.29	0.01	-0.05	0.04	-0.04
0.00	0.00	-363.00	0.00	0.00	0.00	-0.29	-0.29	-363.06	-0.05	0.04	0.00	-0.29	-0.29	-0.06	-0.05	0.04	0.00
0.00	0.00	-353.00	0.00	0.00	0.00	-0.28	-0.28	-353.05	-0.05	0.09	0.00	-0.28	-0.28	-0.05	-0.05	0.09	0.00
20.00	0.00	-373.00	0.00	0.00	0.00	19.39	-0.69	-372.98	-0.22	0.13	-0.06	-0.61	-0.69	0.02	-0.22	0.13	-0.06
20.00	0.00	-363.00	0.00	0.00	0.00	19.56	-0.64	-363.02	-0.08	0.13	-0.06	-0.44	-0.64	-0.02	-0.08	0.13	-0.06
20.00	0.00	-353.00	0.00	0.00	0.00	19.40	-0.90	-353.02	-0.22	0.18	-0.06	-0.60	-0.90	-0.02	-0.22	0.18	-0.06
-20.00	20.00	-373.00	0.00	0.00	0.00	-20.50	19.83	-373.06	0.04	-0.05	0.04	-0.50	-0.17	-0.06	0.04	-0.05	0.04
-20.00	20.00	-363.00	0.00	0.00	0.00	-20.65	19.71	-363.14	0.00	-0.04	0.05	-0.65	-0.29	-0.14	0.00	-0.04	0.05
-20.00	20.00	-353.00	0.00	0.00	0.00	-20.49	19.86	-353.09	0.04	-0.05	0.09	-0.49	-0.14	-0.09	0.04	-0.05	0.09
0.00	20.00	-373.00	0.00	0.00	0.00	-0.55	19.98	-373.00	-0.04	0.05	0.00	-0.55	-0.02	0.00	-0.04	0.05	0.00
0.00	20.00	-363.00	0.00	0.00	0.00	-0.82	19.89	-363.12	-0.04	0.09	0.00	-0.82	-0.11	-0.12	-0.04	0.09	0.00
0.00	20.00	-353.00	0.00	0.00	0.00	-0.77	19.72	-353.14	-0.09	0.05	0.00	-0.77	-0.28	-0.14	-0.09	0.05	0.00
20.00	20.00	-373.00	0.00	0.00	0.00	19.14	19.66	-373.11	-0.18	0.13	-0.06	-0.86	-0.34	-0.11	-0.18	0.13	-0.06
20.00	20.00	-363.00	0.00	0.00	0.00	19.32	19.58	-363.25	-0.18	0.13	-0.06	-0.68	-0.42	-0.25	-0.18	0.13	-0.06
20.00	20.00	-353.00	0.00	0.00	0.00	19.17	19.45	-353.22	-0.18	0.18	-0.06	-0.83	-0.55	-0.22	-0.18	0.18	-0.06
								average of error				-0.52	0.05	-0.07	-0.02	0.08	-0.03
								standard deviation of error				0.21	0.57	0.07	0.14	0.08	0.04

Retrieval Number: 100.1/ijrte.F68400310622
DOI: 10.35940/ijrte.F6840.0310622
Journal Website: www.ijrte.org

Published By:
Blue Eyes Intelligence Engineering
and Sciences Publication (BEIESP)

Table 2 Results of Accuracy Verification in Rotation

ideal value						measured value						error					
x [mm]	y [mm]	z [mm]	α [deg]	β [deg]	γ [deg]	x [mm]	y [mm]	z [mm]	α [deg]	β [deg]	γ [deg]	x [mm]	y [mm]	z [mm]	α [deg]	β [deg]	γ [deg]
0.00	0.00	-373.00	-15.00	-15.00	-20.00	-0.75	-0.66	-372.79	-15.04	-14.87	-15.85	-0.75	-0.66	0.21	-0.04	0.13	4.15
0.00	0.00	-373.00	-15.00	-15.00	0.00	-0.10	-0.19	-373.08	-15.19	-14.75	3.84	-0.10	-0.19	-0.08	-0.19	0.25	3.84
0.00	0.00	-373.00	-15.00	-15.00	20.00	0.06	0.89	-373.14	-14.70	-14.79	23.67	0.06	0.89	-0.14	0.30	0.21	3.67
0.00	0.00	-373.00	0.00	-15.00	-20.00	-0.25	-0.23	-373.05	0.25	-15.07	-20.07	-0.25	-0.23	-0.05	0.25	-0.07	-0.07
0.00	0.00	-373.00	0.00	-15.00	0.00	-0.29	0.15	-373.08	0.57	-14.90	-0.04	-0.29	0.15	-0.08	0.57	0.10	-0.04
0.00	0.00	-373.00	0.00	-15.00	20.00	-0.41	1.43	-373.10	0.87	-14.85	19.87	-0.41	1.43	-0.10	0.87	0.15	-0.13
0.00	0.00	-373.00	15.00	-15.00	-20.00	-0.06	0.76	-373.04	15.87	-14.06	-24.20	-0.06	0.76	-0.04	0.87	0.94	-4.20
0.00	0.00	-373.00	15.00	-15.00	0.00	-0.45	1.67	-373.08	15.89	-14.09	-4.41	-0.45	1.67	-0.08	0.89	0.91	-4.41
0.00	0.00	-373.00	15.00	-15.00	20.00	-1.13	1.95	-373.09	16.09	-13.89	15.87	-1.13	1.95	-0.09	1.09	1.11	-4.13
0.00	0.00	-373.00	-15.00	0.00	-20.00	-0.68	0.43	-372.93	-15.14	-0.37	-19.98	-0.68	0.43	0.07	-0.14	-0.37	0.02
0.00	0.00	-373.00	-15.00	0.00	0.00	-0.35	0.29	-372.99	-14.89	-0.23	0.04	-0.35	0.29	0.01	0.11	-0.23	0.04
0.00	0.00	-373.00	-15.00	0.00	20.00	-0.39	0.76	-373.06	-14.48	-0.20	20.06	-0.39	0.76	-0.06	0.52	-0.20	0.06
0.00	0.00	-373.00	0.00	0.00	-20.00	-0.49	0.65	-373.01	-0.15	-0.10	-20.02	-0.49	0.65	-0.01	-0.15	-0.10	-0.02
0.00	0.00	-373.00	0.00	0.00	0.00	-0.59	0.81	-373.01	0.05	0.09	0.00	-0.59	0.81	-0.01	0.05	0.09	0.00
0.00	0.00	-373.00	0.00	0.00	20.00	-0.75	0.65	-373.00	0.28	0.23	20.03	-0.75	0.65	0.00	0.28	0.23	0.03
0.00	0.00	-373.00	15.00	0.00	-20.00	-0.30	1.17	-373.06	14.87	0.25	-20.31	-0.30	1.17	-0.06	-0.13	0.25	-0.31
0.00	0.00	-373.00	15.00	0.00	0.00	-0.82	1.31	-373.05	14.94	0.44	-0.09	-0.82	1.31	-0.05	-0.06	0.44	-0.09
0.00	0.00	-373.00	15.00	0.00	20.00	-1.08	0.86	-373.01	15.10	0.67	19.87	-1.08	0.86	-0.01	0.10	0.67	-0.13
0.00	0.00	-373.00	-15.00	15.00	-20.00	-1.07	-0.47	-372.79	-16.33	13.61	-24.00	-1.07	-0.47	0.21	-1.33	-1.39	-4.00
0.00	0.00	-373.00	-15.00	15.00	0.00	-0.60	-1.20	-372.78	-16.17	13.86	-3.87	-0.60	-1.20	0.22	-1.17	-1.14	-3.87
0.00	0.00	-373.00	-15.00	15.00	20.00	-0.44	-1.01	-372.68	-15.35	14.06	16.06	-0.44	-1.01	0.32	-0.35	-0.94	-3.94
0.00	0.00	-373.00	0.00	15.00	-20.00	-0.71	0.81	-372.89	-0.74	14.38	-20.32	-0.71	0.81	0.11	-0.74	-0.62	-0.32
0.00	0.00	-373.00	0.00	15.00	0.00	-0.86	0.14	-372.84	-0.56	14.67	-0.16	-0.86	0.14	0.16	-0.56	-0.33	-0.16
0.00	0.00	-373.00	0.00	15.00	20.00	-0.80	-0.82	-372.80	-0.35	14.89	19.82	-0.80	-0.82	0.20	-0.35	-0.11	-0.18
0.00	0.00	-373.00	15.00	15.00	-20.00	-0.34	1.49	-373.08	14.78	14.27	-16.54	-0.34	1.49	-0.08	-0.22	-0.73	3.46
0.00	0.00	-373.00	15.00	15.00	0.00	-0.79	1.14	-372.97	15.00	14.54	3.72	-0.79	1.14	0.03	0.00	-0.46	3.72
0.00	0.00	-373.00	15.00	15.00	20.00	-1.27	-0.61	-372.87	15.13	14.88	23.64	-1.27	-0.61	0.13	0.13	-0.12	3.64
								average of error				-0.58	0.45	0.03	0.02	-0.05	-0.12
								standard deviation of error				0.34	0.86	0.12	0.58	0.60	2.67

As a whole, the average errors and the standard deviation of the errors are small, and it can be seen that a highly accurate measuring instrument has been realized. On the other hand, when looking individually, when comparing the cases of x = -20.0 mm and y = -20.0 mm with those of x = 20.0 mm and y = 20.0 mm in the accuracy verification in translation, the error in the y-axis direction is large and the sign is also inversed. Similarly, in the accuracy verification in rotation, when α = -15.0, 15.0 degree, a large error occurs in γ and the sign is also inverted. For this reason, it is considered that although the measuring instrument itself was machined and assembled with high accuracy, there is a large installation error between the measuring instrument and the 6-axis stage when it is fixed to the frame. In fact, as shown in Figure 10, it can be seen visually that the measuring instrument and the 6-axis stage are not parallel.

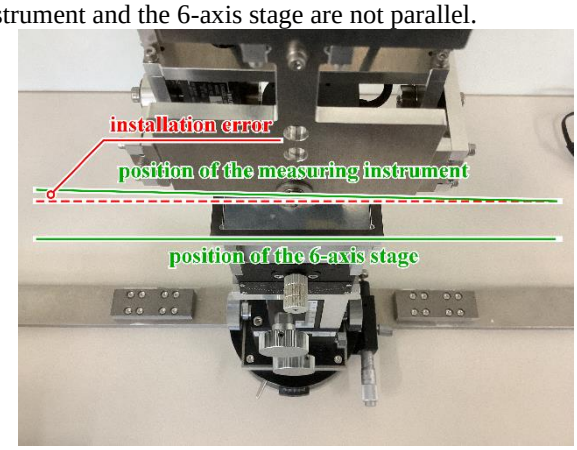

Fig. 10 Installation Error between the Measuring Instrument and the 6-axis Stage

V. CONCLUSION

In this paper, we described a contact-type three-dimensional position measuring instrument for verification of the piping inspection robot, and we proposed the structure of the measuring instrument that does not significantly disturb the driving of the robot due to the disturbance caused via the connection part of the piping inspection robot and the measuring instrument. Furthermore, as a result of experiments, even in the initial state where the accuracy of the measuring instrument is not calibrated, the average translation error is within 0.58 mm, the average angle error is within 0.12 degree, the standard deviation of the translation error is within 0.86 mm, and the standard deviation of the angle error is within 2.67 degree, so that it was shown that it can be used for verification of the robot. In the future, the following two issues will be discussed in order to further improve the accuracy.

1. Calibration of the Contact Type Three-Dimensional Position Measuring Instrument

At present, the measuring instrument itself has achieved high accuracy, but apart from that, it can be seen from the experimental results that there are errors in the inclination as installation errors. Therefore, it is desirable to realize a highly accurate measuring instrument by calibrating the attachment errors, which are external parameters of the errors, in addition to the mechanical errors that occur during processing and assembly of the measuring instrument, which are the internal parameters of the errors.

2. Calibration at the time of installation

In order to actually verify a piping inspection robot, it is necessary to install the measuring instrument on the piping test field. When doing so, attachment errors, which is external parameters of the errors, occur between the piping and the measuring instrument. Therefore, by estimating the external parameters of the errors again using the internal parameters of 1, it is possible to verify the robot in an environment where highly accurate measurement can be performed.

REFERENCES

1. Japan institute of wastewater engineering technology, "Development foundation survey of sewerage facilities management robot", Sewer new technology Annual report of the Institute, 1992, pp.43-52.
2. Rome, E., Hertzberg, J., Kirchner, F., Licht, U. and Christaller, T., "Towards Autonomous Sewer Robots: the MAKRO Project", Urban Water, Vol. 1, 1999, pp. 57-70.
3. Streich, H. and Adria, O., "Software approach for the autonomous inspection robot MAKRO", in Proceedings of the 2004 IEEE International Conference Robotics and Automation, 2004, pp. 3411-3416.
4. Birkenhofer, C., Regenstein, K., Zöllner, J. M. and Dillmann, R., "Architecture of multi-segmented inspection Robot KAIRO-II", DOI: 10.1007/978-1-84628-974-3_35, In book: Robot Motion and Control, 2007, pp.381-389.
5. Hirokazu, U. and Kazuo, I., "Basic research on crack detection for sewer pipe inspection robot using image processing", Proceedings of the 2009 JSME Conference on Robotics and Mechatronics, 2009, 1A1-C02.
6. Ryosuke, I., Yoshikazu, O., Shigeru, K., Yasuhiro, K., Yoshihiro, Y., Sakae, U., Takayuki, K., Hirofumi, M., Toshi, T. and Satoshi, T., "Development of remote control system for search and rescue robot in confined space", 2010 Symposium on System Integration, 2010, pp.1238-1241.
7. Hirofumi, M., Kiyoshi, I., Yoshikazu, O., Shigeru, K. and Toshi, T., "Development of Middleware for Rescue Robots to Facilitate Device Management", Proceedings of the JSME, No.115-1, 2011, p.123-124.
8. Hirofumi, M., Shigeru, K. and Toshi, T., "Development of system for rescue robots to facilitate device management", Bulletin of National Institute of Technology, Yuge College, Vol. 34, 2012, pp.48-53.
9. Ayaka, N., Kazutomo, F., Toshikazu, S., Mikio, G. and Hirofumi M., "Prototype design for a piping inspection robot", 43rd Graduation Research Presentation Lecture of Student Members of the JSME, 2013, 716.
10. Kazutomo, F., Yoshiki, I. and Hirofumi M., "Modularization for a piping inspection robot", 2013 Symposium on System Integration, 2013, pp.1297-1300.
11. Kazutomo, F., Toshikazu, S., Mikio, G., Yoshiki, I. and Hirofumi M., "Miniaturization of the piping inspection robot by modularization", 44rd Graduation Research Presentation Lecture of Student Members of the JSME, 2014, 613.
12. Hirofumi, M., Takuya, K., Kazutomo, F., Yoshiki, I., Toshikazu, S. and Mikio, G., "Research and development about a piping inspection robot - Report1: Prototype design for a miniaturization -", Bulletin of National Institute of Technology, Yuge College, Vol. 36, 2014, pp.79-82.
13. Hirofumi, M., Yoshiki, I., Toshikazu, S. and Mikio, G., "Research and development about a piping inspection robot - Report2: Prototype design for maintenance improvement -", Bulletin of National Institute of Technology, Yuge College, Vol. 37, 2015, pp.75-79.
14. Hirofumi M., Ryota, K., "Development of a small autonomous pipe inspection robot (Modularization of hardware using the technique of wooden mosaic work)", Transactions of the Japan Society of Mechanical Engineers, Vol.82, No.839, 2016, pp.1-16.
15. Hirofumi M., "Automatic Compensation of the Positional Error Utilizing Localization Method in Pipe", International Journal of Recent Technology and Engineering (IJRTE), Vol.9, No.6, 2021, pp.151-157.
16. Yuki, Y., Yoshiki, I., Hirofumi, M., "Self-localization Measurement of the Piping Inspection Robot by a ARtoolkit", Transactions of the Japan Society of Mechanical Engineers, No. 165-1, 2016, 502.
17. Ayano, T., Hirofumi, M., "Accuracy Improvement of the Measuring Instrument for the Piping Inspection Robot", The Japan Society of Mechanical Engineers Chugoku-Shikoku Branch, the 47th Conference on the Graduation Thesis for Undergraduate Students,2017, 921.
18. Ayano, T., Hirofumi, M., "Tilt Adjustment to Measuring Instrument for Piping Inspection Robot", Transactions of the Japan Society of Mechanical Engineers, No. 185-1, 2018, 1304.

AUTHOR PROFILE

Hirofumi Maeda, is Associate Professor in the Information Science and Technology Department at National Institute of Technology (KOSEN), Yuge College. Dr. Maeda's research focuses on practical application of mechanical engineering, namely, developing rescue robots, pipe inspection robots and natural language processing. Dr. Maeda previously served as a researcher at the NPO International Rescue System Institute. Dr. Maeda is currently a member of the Japan Society of Mechanical Engineers, the Robotics Society of Japan, the Japan Association for College of Technology, and the Japan Institute of Marine Engineering. Dr. Maeda has published 10 peer-reviewed papers and presented 78 papers. In addition, Dr. Maeda received two awards at academic conferences and 13 external funds.